Development of event reconstruction algorithm for full-body gamma-camera based on SiPMs

D E Philippov, V N Belyaev, P Zh Buzhan, A L Ilyin, E V Popova* and A A Stifutkin
National Research Nuclear University MEPhI (Moscow Engineering Physics Institute), Kashirskoe highway 31, Moscow, 115409, Russia

E-mail: filippovdima@rambler.ru, buzhan@inbox.ru, *elenap73@mail.ru

Abstract. The gamma-camera is the detector for nuclear medical imaging where the photomultiplier tubes (PMTs) could be replaced by the silicon photomultipliers (SiPMs). Common systems have the energy resolution about 10% and intrinsic spatial resolution about 3 mm (FWHM). In order to achieve the requirement energy and spatial resolution the classical Anger's logic should be modified. In case of a standard monolithic thallium activated sodium iodide scintillator (500x400x10 mm^3) and SiPM readout it could be done with identification of the clusters. We show that this approach has a good results with the simulated data.

1. Introduction

Most of recent R&D projects in the field of gamma-detectors for medical physics use SiPMs. SiPMs attract a particular interest for developers of detectors for nuclear diagnostics (PET or SPECT), because of its small size, good timing resolution and immunity to magnetic fields. Thus the usage of SiPMs instead of traditional PMTs potentially could improve both the spatial and the timing resolution of the systems and also makes possible the simultaneous use of the nuclear and magnetic-resonance imaging.

The gamma-camera is one of the detectors for nuclear diagnostics where the PMTs could be replaced by the SiPMs. The basic requirements for gamma-cameras are the following: the energy resolution about 10% for 140 keV (the most intensive line of Tc-99m); the operation range of energies from 60 to 360 keV and the intrinsic spatial resolution better than 3 mm in full width on a half of maximum (FWHM).

In this paper we discuss the feasibility to design a gamma-camera with a standard monolithic thallium activated sodium iodide scintillator (NaI(Tl), size of 500x400x10 mm^3), array of 6x6 mm^2 Ketek SiPM PM6660 [1] and 64-channel ASIC MAROC3 [2] as readout electronics. The main problem in such a setup is to achieve the energy resolution at least not worse than those for the standard gamma-cameras. To demonstrate that development of such system is possible, its operation should be first simulated. This simulation has to describe the gamma-quanta interactions, light emission and propagation in scintillator, and the main properties of the SiPM. Also the classical Anger's reconstruction method [3] should be modified to implement it for SiPM's array.

2. Simulation setup

The Monte-Carlo simulation of the full-body gamma camera detection unit was performed using Geant4 (G4) [4] libraries. The simulation has been performed for the following conditions:

- scintillator – NaI(Tl) crystal with size of 500x400x10 mm^3;
- white diffuse reflector was on all sides except the output window;
- crystal was placed in aluminium case with thickness of 2 mm.

For simplicity only one wavelength from real scintillation spectra related to maximum was used, so all optical properties of the components and their surfaces were set only for that mono-line. The light yield of NaI(Tl) was set as 38 photons per keV. The decay time was set as 250 ns. The diffuse reflector was simulated with LUT model of Geant4 [5] and «groundteflonair» surface type with the reflection coefficient of 99.9%. The case output window was 2 mm thick glass coupled with array of SiPMs via optical grease (thickness of 50 um). Each SiPM had size of 7.8x6.8x1.75 mm^3, with sensitive area of 6x6 mm^2. The pitch of the SiPM array was 8 mm for X-axis and 7 mm for Y-axis. All dimensions were taken from existing 64-channel matrix of 6x6 mm^2 Ketek SiPMs (assembled at "Pulsar" in Moscow). This matrix represents one module of the further full-body gamma-camera's detector system. Full detector consists of 62x56 SiPMs which cover almost whole surface of the scintillator. The figure 1 presents schematic model of SiPM array (a), light spread in G4 (b) and SiPM G4 volume (c).

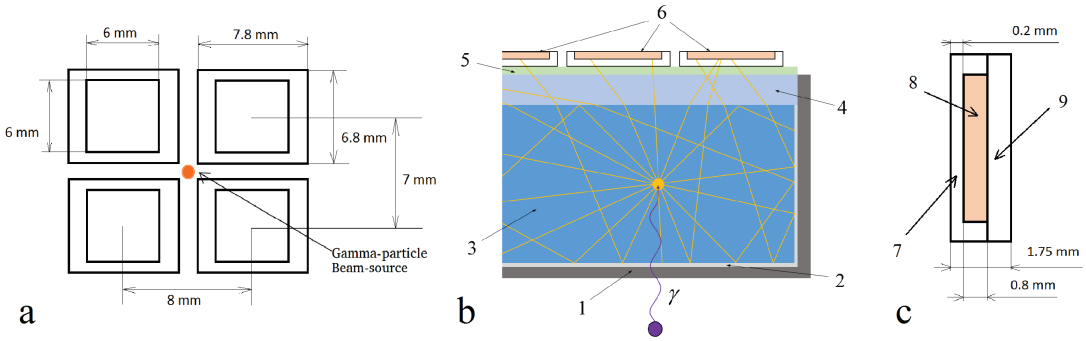

Figure 1. a) four cells from the SiPM array; b) light spread in Geant4; c) SiPM. 1 — aluminium package of the crystal, 2 — diffuse reflector, 3 — NaI(Tl) crystal (n = 1.82), 4 — case output window (n = 1.47), 5 — optical grease (n = 1.51), 6 — photodetector matrix; 7 — epoxy of the SiPM (n = 1.53), 8 — 6x6 mm2 silicon absorbing layer (n = 5.2), 9 — glass-reinforced epoxy laminate FR4 (n = 1.53).

The radionuclide was simulated as a beam point source emitting gamma particles along Z-axis (perpendicular to the detector's surface) with energy of 140 keV at (0;0;50) mm coordinates of world volume in G4 simulation (42 mm from aluminium case).

The output data of G4 simulation was the number of absorbed optical photons in each SiPM for each event. After that G4 data was processed using MATLAB macros to take into account the main properties of SiPMs, such as Dark Counts Rate (DCR) and Photon Detection Efficiency (PDE), and integration time of MAROC3. Thus the number of photons first was converted into number of photoelectrons (or fired microcells, not saturation range) with binomial distribution of PDE of 40% and integration time of 150 ns, and then Poisson distributed dark counts with the rate 14 MHz were added to the signal of each SiPM. Therefore the mean DCR was 2.1 count per event per SiPM and total conversion efficiency of the system (for absorbed light photons) was about 19%.

3. Methods

The final data was processed with three algorithms to reconstruct energy and position information:

- simple Anger's logic with the threshold;
- modified Anger's logic with the threshold and adaptive variable radius;
- modified Anger's logic with the threshold and static cluster's size of N-by-N SiPMs.

3.1. Simple Anger's logic with the threshold

The first algorithm is the standard Anger's logic. The signals above the threshold were used to reconstruct event energy and position, using center-of-gravity formulas (1) for all triggered detectors:

$$\bar{x} = \sum_{i=1}^{N} x_i \cdot A_i \cdot (\sum_{i=1}^{N} A_i)^{-1} \qquad \bar{y} = \sum_{i=1}^{N} y_i \cdot A_i \cdot (\sum_{i=1}^{N} A_i)^{-1} \qquad Energy = \sum_{i=1}^{N} A_i \ , \tag{1}$$

where x_i, y_i - (x;y)-coordinates of i-photodetector, A_i – corresponding amplitude and $\bar{x}$, $\bar{y}$ - center of gravity position.

3.2. Modified Anger's logic with threshold and adaptive variable radius

In the second algorithm the primary cluster was determined as in the first one. All signals from detectors those above the threshold were used to calculate cluster's center coordinates (CCC) using (1) and the standard deviations (σ_x and σ_y) using statistical formulas for discrete distributions (2):

$$\sigma_X = [\sum_{i=1}^{N} (x_i - \bar{x})^2 \cdot A_i \cdot (\sum_{i=1}^{N} A_i)^{-1}]^{1/2} \qquad \sigma_Y = [\sum_{i=1}^{N} (y_i - \bar{y})^2 \cdot A_i \cdot (\sum_{i=1}^{N} A_i)^{-1}]^{1/2} \ . \tag{2}$$

After that the average value of σ_x and σ_y was multiplied by numerical coefficient C and labeled as the cluster's radius. Thus the cluster's radius changes according to width of signals distribution. The signals of the detectors which centers lay inside the cluster were used to get position and energy information using center of gravity formulas (1) again.

3.3. Modified Anger's logic with threshold and static cluster's size of N-by-N SiPMs

The third method differs from second in how the cluster size is defined. Here it was defined as the rectangular arrays of N-by-N SiPMs instead of σ with CCC determined exactly as for the previous method.

4. Results

After the simulated data (from gamma source mentioned above) were processed using all algorithms the following results have been obtained. The energy resolution for the first algorithm was 26.7% without threshold, and 19% and 22.6% with threshold of 5 and 10 photoelectrons (phe), respectively (figure 2a). The plots of the spatial and energy resolution changes versus threshold value for the first algorithm are shown in figure 2b.

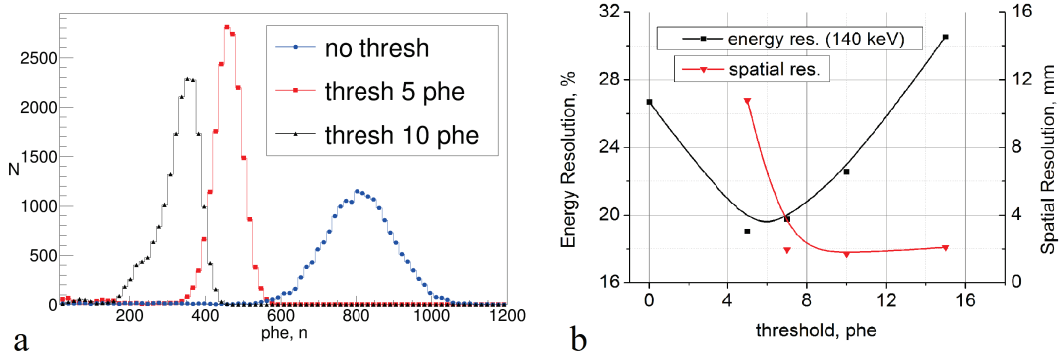

Figure 2. First algorithm, a) energy spectra, thresholds of 0, 5 and 10 phe; b) energy and spatial resolution versus threshold (solid line – b-spline interpolation).

The first algorithm can't be used for the position reconstruction without threshold, but the spatial resolution of 10.8 and 1.7 mm (FWHM) have been obtained for the thresholds of 5 phe and 10 phe, respectively (figure 3).

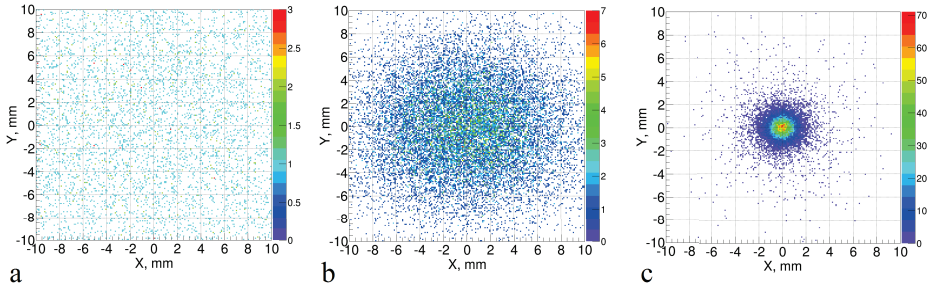

Figure 3. First algorithm. The distribution of reconstructed positions from point source for different thresholds: a) 0 phe; b) 5 phe; c) 10 phe.

The threshold values of 5 and 10 phe had been also used for reconstruction using the second algorithm. The mean value σ_5 was 35.6 mm for the threshold of 5 phe, and the mean value σ_{10} was 6.6 mm for the threshold of 10 phe (figure 4a).

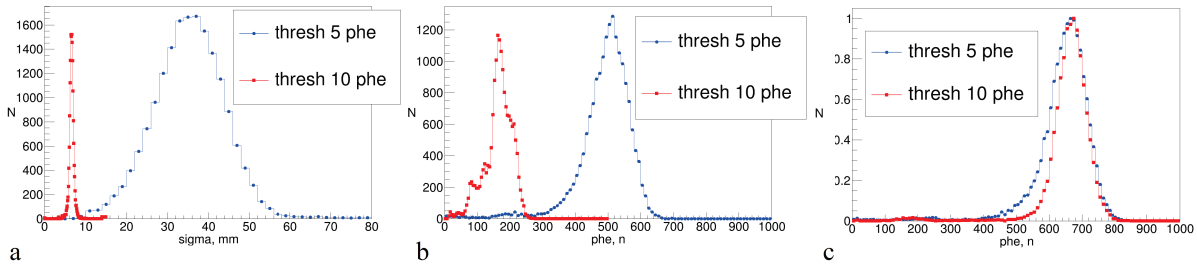

Figure 4. Second algorithm, a) distribution of averaged by X and Y standard deviation for thresholds of 5 and 10 phe; b) the energy spectra for the thresholds of 5 and 10 phe, radii $1\sigma_5$ and $1\sigma_{10}$; c) radii $2\sigma_5$ and $11\sigma_{10}$ (normalized spectra).

The energy spectra have a distortion of the photopeak (figure 4b) for the clusters, which radius was determined as 1σ (σ_5 and σ_{10}, respectively). Especially, this is clearly seen for the 10 phe threshold. The energy spectra (normalized) are shown in figure 4c with the best energy resolutions of the equal cluster's size for both thresholds (radii $2\sigma_5$ and $11\sigma_{10}$).

Thus for the threshold of 5 phe the optimal radius for the best energy resolution was $2\sigma_5$, and corresponding energy resolution was 18.1%. For the threshold of 10 phe the best energy resolution has been obtained of about 14.9% with the 8-$11\sigma_{10}$ radii. The plots of the spatial and energy resolution as function of the radius (in mm) are given in figure 5 for the thresholds of 5 and 10 phe. The best spatial resolution for the second algorithm was obtained with $1\sigma_5$ and $3\sigma_{10}$ radii and amounted to 3 mm and 1.5 mm, respectively for two thresholds.

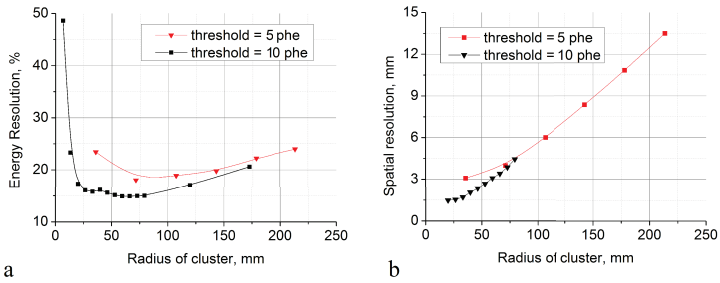

Figure 5. Second algorithm, a) the energy resolution versus the radius; b) the spatial resolution versus the radius (solid line – b-spline interpolation).

For the third algorithm the energy and spatial resolution dependencies on the cluster size was obtained for the threshold of 10 phe, since this threshold in the second algorithm provides the best energy resolution. In figure 6a, the spatial and energy resolution dependencies on cluster size are plotted. As seen on the graph, the best energy resolution of 12.8% of all three algorithms was obtained for the cluster size of 12x12 SiPM. At the same time the best spatial resolution of 1.35 mm was obtained for the 6x6 cluster, while the energy resolution for that cluster was 16.1% (figure 6b).

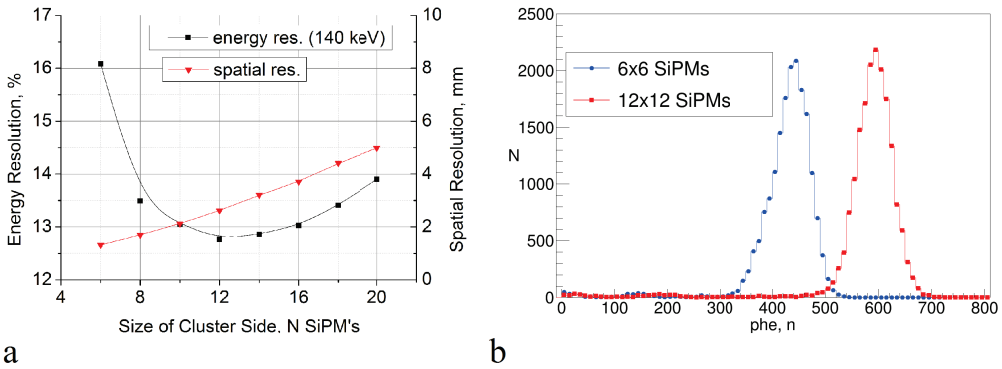

Figure 6. Third algorithm, a) energy and spatial resolution versus cluster's size (N-by-N SiPMs) for the threshold of 10 pe (solid line – b-spline interpolation); b) energy spectra for clusters 6x6 and 12x12 SiPM's.

Additionally, events were generated when the beam source (140 keV) was uniformly distributed over the detector surface. 2D distributions of the reconstructed event's positions for all algorithms are shown in figure 7. The results are shown only for the one detector quadrant in order to reduce the time of the data processing, due to the geometry's symmetry for both X and Y axis.

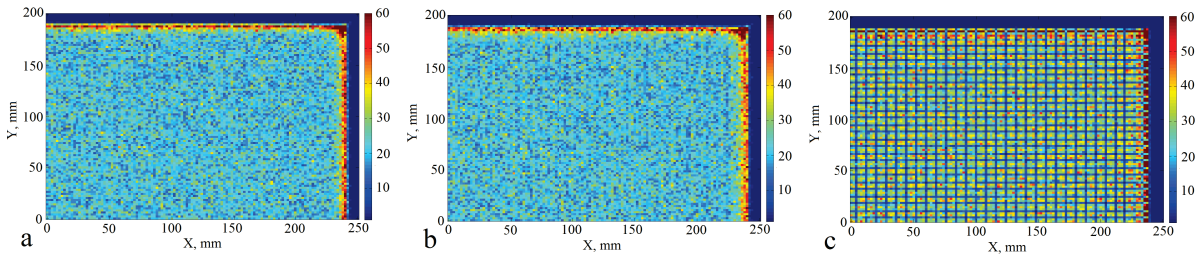

Figure 7. The distribution of reconstructed event's positions from uniformly distributed source (140 keV), threshold of 10 pe. a) first algorithm; b) second algorithm with $3\sigma_{10}$ radius; c) third algorithm with 12x12 SiPM cluster size.

5. Results discussion

5.1. Energy resolution

According to the results, it is not possible to achieve good energy resolution using the standard Anger logic (first method), since the sum of the signals from all the photodetectors increases significantly the noise contribution in the energy resolution. The threshold helps to skip over the detectors whose signal have no useful information, but when the threshold increases, the SiPMs cluster loses useful information and that leads to distortion of the energy spectrum and to the worse energy resolution. Thus, the using of the only one threshold is rather crude approach and insufficient to determine the optimal cluster.

The second and the third methods apply preliminary procedure to define cluster position and size and after that carry on reconstruction using selected devices. It allows to obtain much better results than in the first method. The fixed size rectangular cluster (algorithm 3) providing the highest energy resolution for given detector's geometry. However, such optimization is not sufficient to achieve the required energy resolution of 10%. The improvement of the photodetector parameters is also needed.

5.2. Spatial resolution

The enhancement of the intrinsic resolution is one of the advantages of the SiPM based gamma-camera. According to the results of simulation additional clarification in the cluster selection does not significantly improve the spatial resolution. Thus the spatial resolution unlike the energy one is less affected by influence of the DCR and the only threshold approach is sufficient for the position reconstruction. Also worth noting that the distributions of the reconstructed coordinates from the uniformly distributed source (figure 7) show the uniformity of the first and second methods throughout the plane of the crystal (except the regions close to the edges), unlike the third algorithm, whose response depends on the location of the interaction point relative to the SiPM.

6. Conclusion

The operation of the detection module of the full-body gamma-camera which consists of the monolithic sodium iodide crystal, array of the SiPMs and was irradiated by 140 keV beam point source was simulated. The simulation also includes two main SiPM parameters: the dark count rate and the photon detection efficiency, as well as the integration time of the readout electronics. The results of the position and energy data reconstructions using three algorithms based on the Anger logic are presented.

The major improvement of the suggested reconstruction methods is in the finding of the signal cluster for the further energy and coordinates calculations using centre of gravity formulas (1). The best energy resolution was 12.8% for 140 keV. The best spatial resolution amounted to 1.5 mm (FWHM).

The obtained results show feasibility of the creation of the full-body gamma-camera based on SiPM.

Acknowledgments

This work was supported by Megagrant 2013 program of Russia, agreement №14.A12.31.0006 from 24.06.2013 and partially supported by MEPhI Academic Excellence Project (contract № 02.a03.21.0005, 27.08.2013).

References

[1] PM6660 SiPM Ketek (*http://www.ketek.net/products/sipm/pm6660/)*
[2] ASIC Maroc3 (*http://omega.in2p3.fr/index.php/products/maroc-front-end-chip.html*)
[3] Peterson T and Furenlid L 2011 *Phys. Med. Biol.* **56** R154
[4] Agostinelli S *et al.* 2003 *Nucl. Instr. Meth.* A **506** 252-3
[5] Janecek M and Moses W. 2010 *IEEE Trans. Nucl. Sci.* **57** 967
[6] MATLAB (*www.mathworks.com*)